



NJC

The Improved Hydrodechlorination Catalytic Reactions by Concerted Efforts of Ionic Liquid and Activated Carbon Support.

Journal:	<i>New Journal of Chemistry</i>
Manuscript ID	NJ-ART-01-2019-000273.R1
Article Type:	Paper
Date Submitted by the Author:	16-Mar-2019
Complete List of Authors:	<p>Li, Rongrong; Zhejiang University of Technology, Industrial Catalysis Institute of Zhejiang University of Technology; School of Pharmaceutical and Chemical Engineering</p> <p>Zhou, Ze hua; School of Pharmaceutical and Materials Engineering, TaiZhou University, Taizhou, Zhejiang 318000, PR China.,</p> <p>Chen, Jingjing; School of Pharmaceutical and Materials Engineering, TaiZhou University, Taizhou, Zhejiang 318000, PR China.</p> <p>Wang, Shiting; School of Pharmaceutical and Materials Engineering, TaiZhou University, Taizhou, Zhejiang 318000, PR China.</p> <p>Zheng, Jianli; School of Pharmaceutical and Materials Engineering, TaiZhou University, Taizhou, Zhejiang 318000, PR China.</p> <p>Chu, Chu; School of Pharmaceutical and Materials Engineering, TaiZhou University, Taizhou, Zhejiang 318000, PR China.</p> <p>Zhao, Jia; Zhejiang University of Technology, college of chemical engineering</p> <p>Fan, Hau-Jun; Prairie View A&M University, Chemistry</p> <p>han, deman; school of pharmaceutical and chemical engineering, taizhou university</p>

SCHOLARONE™
Manuscripts

The Improved Hydrodechlorination Catalytic Reactions by Concerted Efforts of Ionic Liquid and Activated Carbon Support

Rongrong Li^{1, *}, Zehua Zhou¹, Jingjing Chen¹, Shiting Wang¹, Jianli Zheng¹, Chu Chu¹, Jia Zhao², Huajun Fan^{3, *}, Deman Han^{1, *}

¹ School of Pharmaceutical and Materials Engineering, TaiZhou University, Taizhou, Zhejiang 318000, PR China.

² Industrial Catalysis Institute of Zhejiang University of Technology, Hangzhou, 310014, P.R. China.

³ Department of Chemistry, Prairie View A&M University, Prairie View, Texas 77446, USA.

*Corresponding Authors:

*Tel.: +86 576 88660353. E-mail: lrr@tzc.edu.cn (Rongrong Li)

*Tel.: +86 576 88660177. E-mail: hdm@tzc.edu.cn (Deman Han).

*Tel.: (936) 261-3111. E-mail: hjfan@pvamu.edu (Huajun Fan).

Abstract

The modified and stabilized palladium nanoparticles were prepared successfully by using the ionic liquid, 1-butyl-3-methylimidazolium trifluoroacetate. The activated carbon was used as the support for the palladium catalyst. Instead of using hydrogen

1
2
3
4 22 gas, the Pd-catalyzed hydrodechlorination (HDC) reaction in this study used aqueous
5
6 23 formic acid-formate buffer solutions as a hydrogen source for its non-flammability.
7
8
9 24 The results showed that both the ionic liquid and active carbon support facilitate Pd
10
11 25 active center to effectively carry out the catalytic HDC reaction of 4-chlorophenol
12
13 26 (4-CP). The ionic liquid (IL) played a dual role as both solvents and as co-factor to
14
15 27 facilitate the reaction. The IL would stabilize, better disperse, and prevent the
16
17 28 congregation of palladium nanoparticles. On the other hand, the active carbon
18
19 29 provides a stronger binding site for stabilizing the active Pd centers. The catalytic
20
21 30 HDC reaction indicated that the turn over frequency (TOF) of ionic liquid with
22
23 31 reduced catalyst was about 5~6 times higher than that of the non-ionic liquid
24
25 32 mediated catalyst. This excellent catalytic activity suggested that the ionic liquid is
26
27 33 dispersing nanoparticles effectively, preventing the creation of Pd nanoparticles
28
29 34 cluster through the strong interaction Pd species with ionic liquid (IL). This IL-Pd
30
31 35 interaction helped form a protection layer to stabilize the Pd active centers. This study
32
33 36 also confirmed that the both Pd⁰ and Pdⁿ⁺ states were required for the catalytic HDC
34
35 37 reaction. Furthermore, the Pd-catalyst were characterized by different techniques such
36
37 38 as Brunauer–Emmett–Telle (BET) surface area analysis, X-ray photoelectron
38
39 39 spectroscopy, Transmission electron microscopy (TEM) and Fourier-transform
39
40 40 infrared spectroscopy (FT-IR).
40
41
42
43
44
45
46
47
48
49
50
51
52
53
54
55
56
57
58
59
60

42 **Keywords:** Ionic liquids; 4-Chlorophenol; Hydrodechlorination; Formic acid

45

46 **1 Introduction**

47 Chlorinated aromatic hydrocarbons, chlorinated alkanes, olefins, organochlorine
48 pesticides, and other chlorine-containing organic compounds are important chemical
49 raw materials and organic solvents, which are widely used in medicine, leather,
50 electronics and pesticide industries. The waste and by-products in the production and
51 use process pose a threat to the environment and human health. Most of the
52 chlorophenols (CP) are difficult to degrade and bioaccumulate in a long time.
53 Therefore, the degradation of organic chlorides has been a research hotspot in recent
54 years. Catalytic hydrodechlorination (HDC) of organic chlorides is an ideal way to
55 degrade chlorophenols.^{1,2,3} The Pd has been commonly used as a hydrodechlorination
56 catalyst because it is more active than Pt and Rh.⁴⁻⁷ However, the produced chloride
57 by the dechlorination reaction was strongly bound at the active Pd sites that cause the
58 catalyst quickly to lose its catalytic capability.⁸ Furthermore, such adsorption also
59 triggered the aggregation and carbon deposition onto the Pd sites, which further
60 aggravate the deactivation of the catalyst.⁹ Therefore, it is critical to improving the
61 stability of Pd active center in the HDC reaction.

62 Gomez-Sainero et al.¹⁰ suggested the synergism between the active center of the
63 hydrodechlorination reaction between two valence states of Pdⁿ⁺ and Pd⁰. It was
64 suggested that Pdⁿ⁺ species would adsorb activated chlorine molecules to form
65 nucleophilic Cl⁻; while Pd⁰ adsorbs the activated H₂ molecules to form Pd-H bonds.
66 The Pd-H active center then can react with nucleophilic Cl⁻ to complete the

1
2
3
4 67 dechlorination reaction. One can see that the stabilization of this Pd species and active
5
6
7 68 center is the key to maintain an effective catalytic activity.

8
9 69 Recent progress demonstrated that the ionic liquid (IL) compounds possess the
10
11
12 70 unique property such as very low vapor pressure, good solubility, high water thermal
13
14 71 stability and adjustable acid strength.¹¹ These properties are beneficial to the catalytic
15
16
17 72 reaction of metal nanomaterials and reactive solvents. Particularly, the IL layer
18
19
20 73 formed by the liquid on the surface of the carrier can make the Pd active nanoparticles
21
22
23 74 dispersed more uniform. For example, the Pd particle size in the IL-palladium-based
24
25 75 catalyst decreased from 17 nm to the range of 2.8-4.0 nm.¹² Claus and other^{13, 14} found
26
27 76 that [BMIM][N(CN)₂] or [BMIM][NTf₂] can form a Pd complex with 3d⁵/2 state.
28
29
30 77 Such Pd complex can modulate the electron binding energy at the Pd center. The
31
32
33 78 increased binding energy subsequently improve the catalytic activity and stability of
34
35 79 the catalyst.^{15,16} However, IL also has its shortcomings such as low recovery rate due
36
37
38 80 to a loss in the liquid phase of the reaction. To remedy this loss and low recovery,
39
40
41 81 Wasserscheid and others^{17, 18} investigated to improve the stability of IL by modifying
42
43
44 82 the carrier and adding the functional groups to form a more stable bond. Alternatively,
45
46 83 activated carbon (AC) was widely used in HDC reaction for its large pores volume
47
48
49 84 and specific surface area. These characteristics of AC can provide more active
50
51 85 catalytic binding sites on the surface and thus facilitate the catalytic reaction.¹⁰

52
53 86 In this study, the IL mediated palladium catalyst supported by the activated carbon
54
55
56 87 (Pd-IL/AC-cr) will be synthesized and tested its catalytic property towards the
57
58
59 88 hydrodechlorination (HDC) of 4-chlorophenol (4-CP). "cr" stands for the catalyst
60

1
2
3
4 89 which was treated by calcination and reduction. For comparison, both Pd/AC and
5
6 90 Pd-IL/AC-c also be synthesized. We adopted aqueous formic acid-formate solutions
7
8
9 91 as hydrogen source¹⁵ since it is a non-flammable hydrogen source. The catalyst will
10
11 92 be characterized by Brunauer–Emmett–Telle (BET) surface area analysis, X-ray
12
13 93 photoelectron spectroscopy (XPS), transmission electron microscopy (TEM) and
14
15 94 fourier-transform infrared spectroscopy (FT-IR), and catalytic properties such as turn
16
17 95 over frequency (TOF) values will be monitored and compared.
18
19
20
21
22
23

96

97 **2 Experimental**

24
25
26
27 98 The detailed synthesis procedures and chemicals used has been published by the
28
29 99 author in the supporting information section of previous published work.²⁰
30
31
32
33

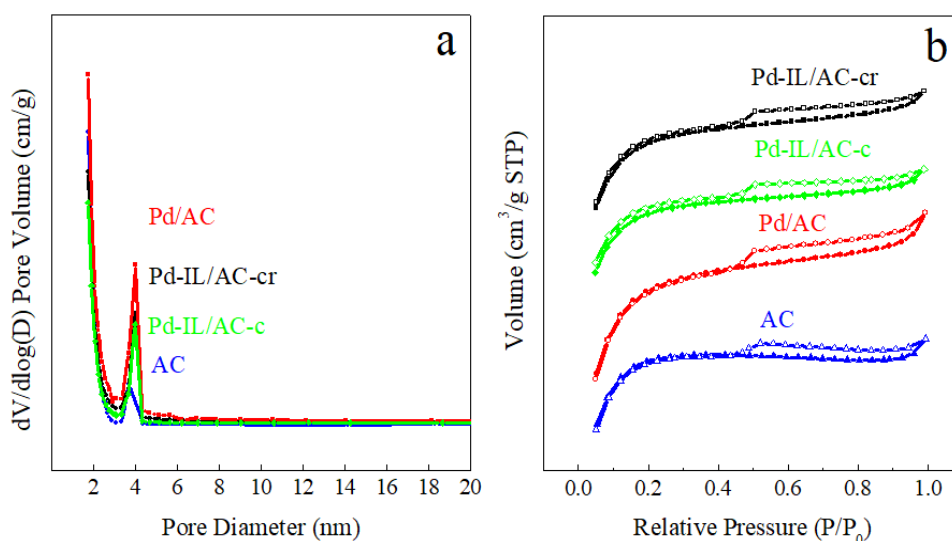
100

101 **3 Results and discussion**

102 **3.1 Catalysts characterization**

34
35
36
37
38
39
40
41 103 Table. 1 summarizes the characterization of the prepared catalysts Pd/AC,
42
43 104 Pd-IL/AC-c and Pd-IL/AC-cr. For comparison and blank test, active carbon (AC) is
44
45
46 105 also listed in the Table. AC is an essentially microporous solid with a high BET
47
48 106 surface of 1209 m² g⁻¹, containing micropores and mesopores within a broad
49
50 107 distribution between 3.5 and 4.5 nm as shown in Fig 1(a). However, the Pd loading
51
52 108 seems to have little effect on the surface area. For example, the Pd deposited complex
53
54
55 109 Pd/AC has slight larger BET surface of 1411 m² g⁻¹, while the BET surface decreases
56
57
58 110 slightly with IL mediated complex Pd-IL/AC-cr and Pd-IL/AC-c to 951 and 921 m²
59
60

1
2
3
4 111 g^{-1} , respectively. This decrease probably is due to the partial collapse of the pores
5
6 112 induced by IL modification through the equivalent-volume impregnation process. Fig
7
8
9 113 1(b) demonstrates the BJH pore distribution curves of catalysts, which have an
10
11
12 114 obvious condensation step at relative pressures $P/P_0 = 0.4\text{--}0.6$. It can be seen from
13
14 115 the shape of the hysteresis loop of Fig. 1 (b) that the pore structure is a tubular pore
15
16 116 structure with both ends open, and the pore diameter is relatively uniform. In general,
17
18
19 117 this open pore structure facilitates the diffusion of molecules, facilitates the adsorption
20
21
22 118 of the reactant molecules on the inner surface and the desorption of the product
23
24
25 119 molecules, thus facilitating the reaction.



120
121 **Fig. 1** (a) the pore size distribution plots of catalysts, (b) the BJH pore distribution curve.

129 **Table. 1** Characterization of the catalysts.

Material	BET surface area (m ² g ⁻¹)	Pore volume (cm ³ g ⁻¹)	Pore Size (nm)	Pd(% wt.) ^a	Pd(% wt.) ^b	Pd ⁰ /Pd ⁿ⁺
AC	1209	0.58	1.92	--	--	--
Pd/AC	1411	0.72	2.06	0.23	0.22	1.02
Pd-IL/AC-cr	951	0.49	2.08	0.54	0.52	1.43
Pd-IL/AC-c	921	0.45	2.07	0.52	0.49	0

130 ^a By the analysis of XPS characterization.131 ^b By the analysis of ICP-MS.

132

133 Previous studies have demonstrated that the HDC reaction can be influenced by the
 134 oxidation state of the Pd centers of the catalyst.^{10,21} Therefore, the surface atomic
 135 composition of Pd-IL/AC-cr was examined by XPS (Fig. 2a) and the detail XPS of C,
 136 N and Pd region are shown in Fig 2b-2d). The content of C, N, Pd and O for
 137 Pd-IL/AC-cr are found to be 85.34%, 1.93%, 0.54%, and 12.18%, respectively. In Fig
 138 2b, we can find XPS bands of C=O, C-O and C-C bonds. The C=O and C-O species
 139 are probably due to the addition of ionic liquids. The N 1s spectrum of Pd-IL/AC-cr
 140 (Fig. 2c) was fitted with two components, which could be attributed to pyridinic-N
 141 (398.9 eV), pyrrolic-N (400.8 eV).²⁵ This doublet in XPS is again due to the
 142 introduction of ionic liquids.

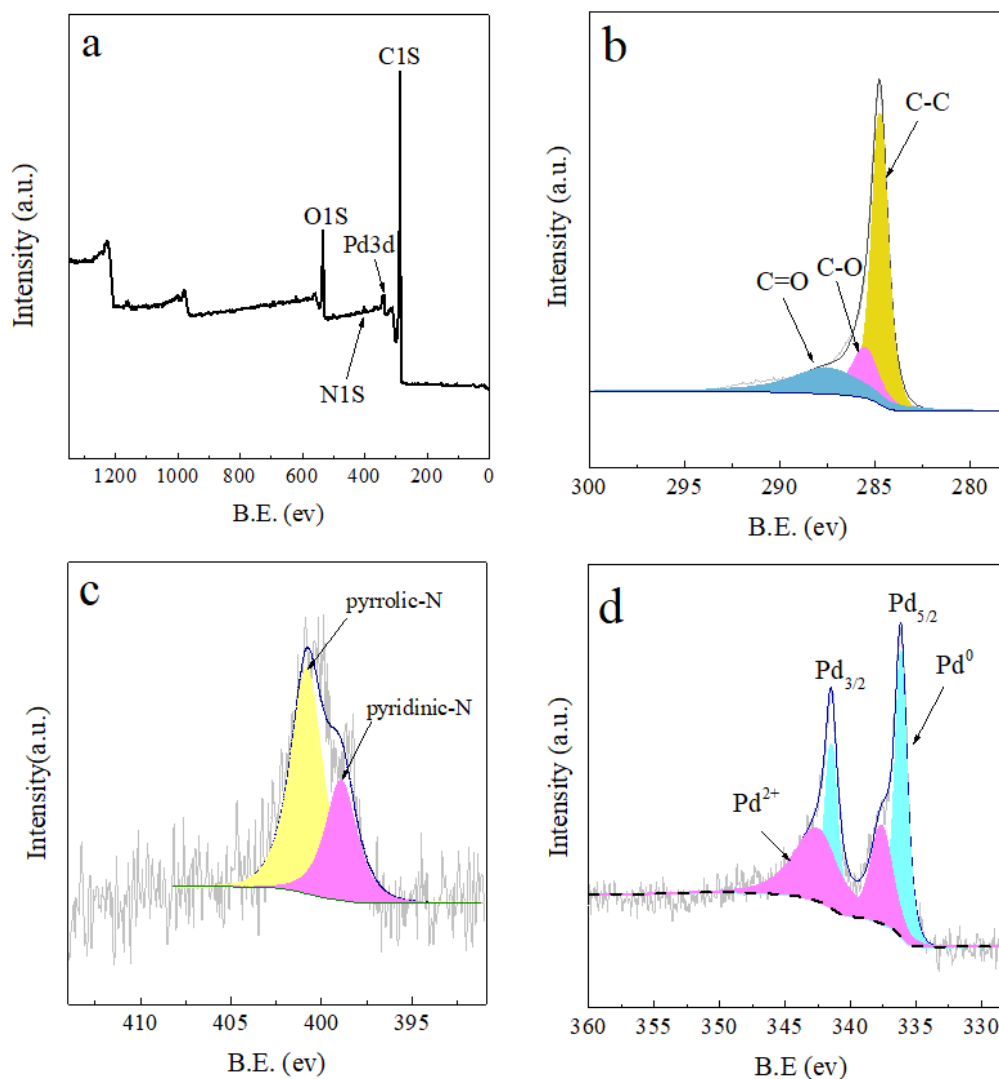


Fig. 2 XPS of Pd-IL/AC-cr. (a) Infrared wide spectrum, (b) C1s, (c) N1s and (d) Pd3d.

Both Pd⁰ and Pdⁿ⁺ species were found in Fig. 2(d). The XPS spectra of Pd 3d have a doublet attributed to Pd 3d_{5/2} and 3d_{3/2}. The Pd 3d_{5/2} peaks at 336.2 eV and 337.0 eV correspond to Pd⁰ and Pd²⁺ species, respectively; while the Pd 3d_{3/2} peaks at 341.4 eV and 342.8 eV correspond to Pd⁰ and Pd²⁺ species, respectively. A previous study²⁴ showed that the binding energy of the Pd 3d_{5/2} of the Pd⁰ is expected to be at 334.9 eV for bulk Pd. In this work, the binding energy for Pd⁰ components of the Pd 3d_{5/2} of Pd-IL/AC-cr catalyst was found to be 336.2 eV, 1.3 eV higher than that of

1
2
3
4 153 bulk Pd. It is interesting to point out that the IL supported catalysts have a higher
5
6 154 content of palladium species (0.54%w.t. for Pd-IL/AC-cr and 0.52%w.t. for
7
8
9 155 Pd-IL/AC-c) than non-IL (0.23%w.t. for Pd/AC) as seen in Table. 1. XPS also reveals
10
11 156 that the Pd⁰/Pdⁿ⁺ ratio increases from 1.02 of Pd/AC to 1.43 of Pd-IL/AC-cr. This
12
13
14 157 might be due to the strong interaction between the anions in IL and the Pd species. All
15
16
17 158 of these factors contribute to the improved catalytic HDC conversion reaction shown
18
19
20 159 in the following “3.2 Activity of the catalysts” section.

21
22 160 The Transmission electron microscopy (TEM) images are utilized to demonstrate
23
24 161 the effect of IL on the dispersion of nanoparticle. The TEM results of Pd/AC (a-1, a-2)
25
26
27 162 and Pd-IL/AC-cr (b-1, b-2) are shown in Fig. 3. Comparing with the TEM images of
28
29
30 163 Pd/AC, one can see the smooth nature of the Pd-IL/AC-cr catalyst surface. The
31
32
33 164 smooth surface of Pd-IL/AC-cr catalyst suggests a more homogeneous dispersion of
34
35
36 165 Pd of Pd-IL/AC-cr catalyst onto the active carbon surface. The Pd nanoparticles’
37
38 166 average size is estimated at 3 nm, which is comparable to the previous study.¹⁰

39
40 167
41
42
43
44
45
46
47
48
49
50
51
52
53
54
55
56
57
58
59
60

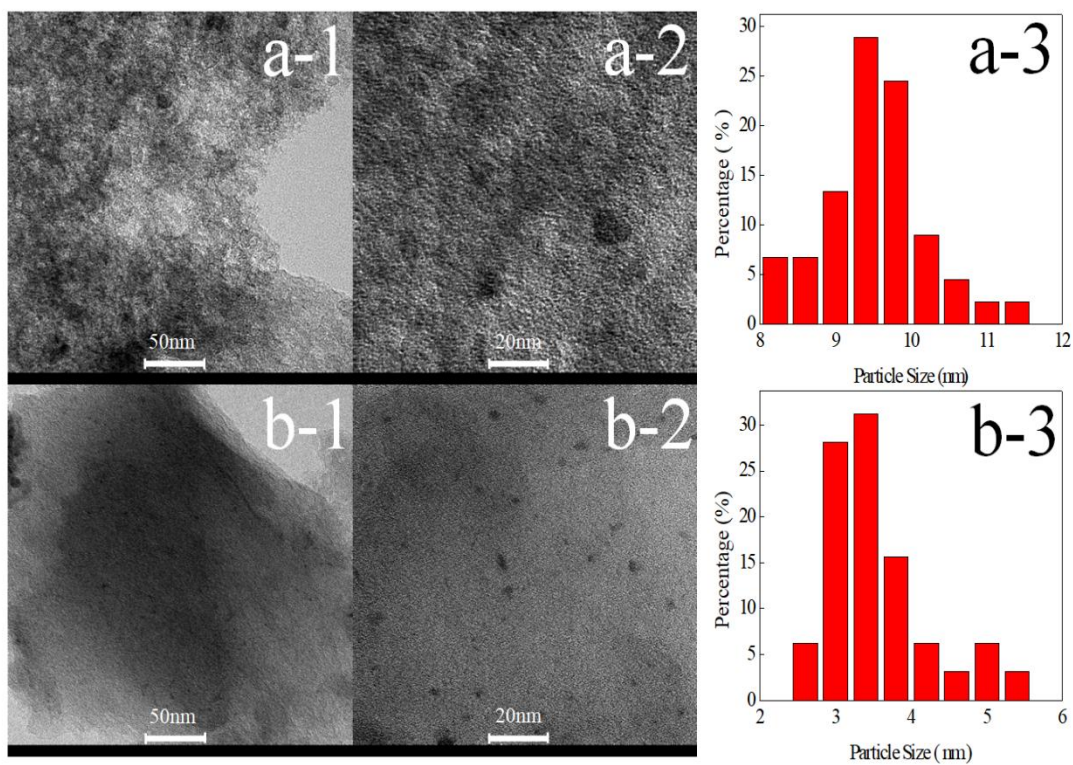


Fig. 3 The TEM image of the Pd/AC (a-1, a-2) and Pd-IL/AC-cr (b-1, b-2) and particle size distribution of the Pd/AC (a-3) and Pd-IL/AC-cr (b-3).

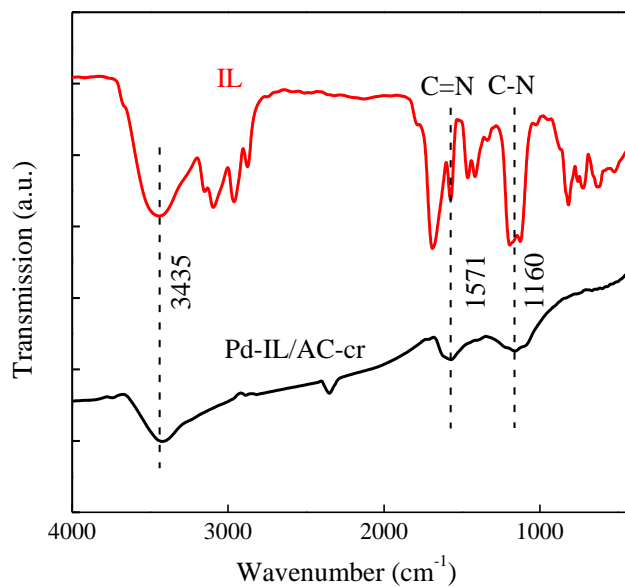


Fig. 4 The FTIR spectra of IL and Pd-IL/AC-cr.

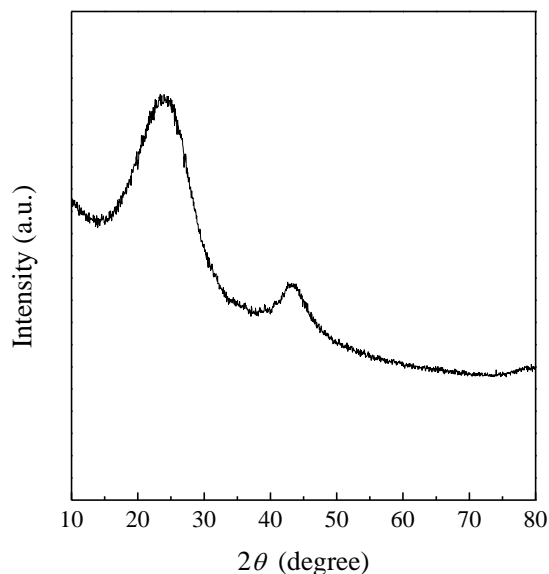


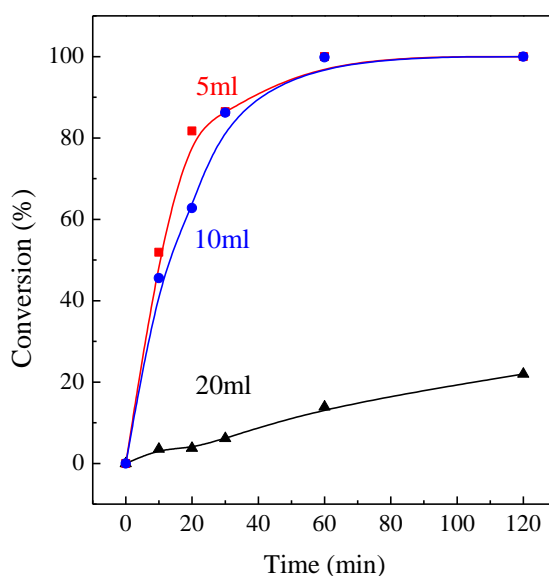
Fig. 5 The X-ray diffraction of Pd-IL/AC-cr.

To examine the binding of the IL on the catalyst, the FTIR spectra of IL and Pd-IL/AC-cr were shown in Fig. 4. The peaks at 1571 cm^{-1} and 1160 cm^{-1} were assigned to C=N and C-N stretching vibrations of IL, respectively, and the broad peak at 3435 cm^{-1} was assigned to N-H stretching. Comparing the FTIR of IL (red in the Fig. 4), the FTIR spectra profile of catalyst indicates that the IL had been successfully loaded on the surface of the catalyst.²⁶ And the X-ray diffraction of Pd-IL/AC-cr (Fig. 5) also shows that the Pd nanoparticles are so small that no diffraction peaks appear.

3.2 Activity of the catalysts

The catalytic property of the prepared catalysts Pd/AC, Pd-IL/AC-cr, and Pd-IL/AC-c was investigated by the hydrodechlorination (HDC) reaction of 4-chlorophenol (4-CP). We first investigated the effect of initial 4-CP concentration

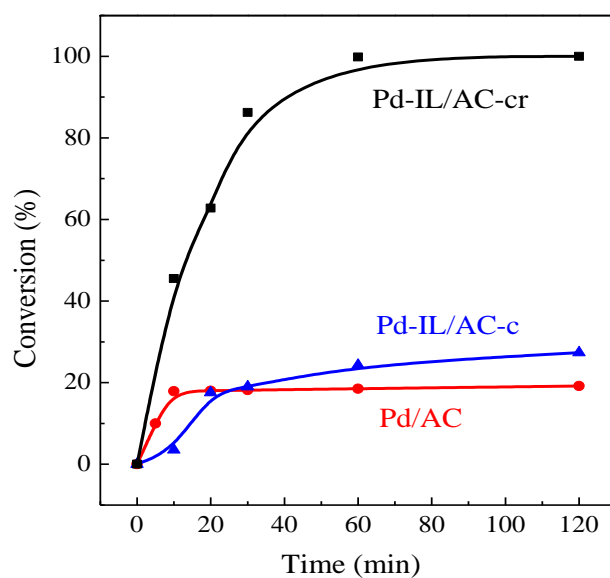
1
2
3
4 189 on the HDC reaction. 0.050 g of Pd-IL/AC-cr catalyst was used in the formic
5
6
7 190 acid-sodium formate buffer solution as the source of hydrogen. The reaction time, the
8
9
10 191 reaction temperature, and stirring rate were set at 2.0 h, 306 K, and 600 rpm,
11
12 192 respectively. As shown in Fig. 6, the reaction conversion percentile with 20 mL of
13
14 193 4-CP was drastically different than those of 10 mL or 5 mL of 4-CP. The higher
15
16 194 concentration (20 mL) of 4-CP seems to yield HDC reaction in much slower pace
17
18 195 over the period and only reached ~20% conversion rate over the 2-hour reaction time.
19
20 196 However, the two lower concentration trials (10 mL and 5 mL) would quickly reach
21
22 197 the 90% mass conversion of 4-CP in the first 30 min and closer to 100% mass
23
24 198 conversion around 1 hour. This suggested that the diffusion effect is effectively
25
26 199 eliminated with the lower 4-CP concentration under the current reaction conditions.
27
28 200 Therefore, it is safe to rule out the mass transfer limitation under the current
29
30
31
32
33
34
35 201 experimental conditions.²⁵



202
203 **Fig. 6** The catalytic HDC of 4-CP at varied initial 4-CP concentrations using Pd-IL/AC-cr.

1
2
3
4 227 study that the different Pd states (Pd^0 and Pd^{n+}) are important to the HDC reaction.²¹
5
6 228 Compared to several other modification methods, our catalysts are more reactive.²²,
7
8
9 229 ²³And the catalyst Pd-IL/AC-cr is still stable in multiple cycles of use, which also
10
11 230 proves that IL has a great effect on the stability of Pd active centers.(Fig. 8)
12
13

14 231



15 232

16 233 **Fig. 7.** The conversion of the catalyst Pd-IL/AC-cr and Pd-IL/AC-c and Pd/AC.

17 234 Reaction conditions: 0.05 g catalyst, 10 mL (8 g/L, 4-CP) + 10 mL (1 mol/L HCOOH + 0.8 mol/L HCOONa), Time = 2 h, Temperature =

18 235

306 K, Stirring rate = 600 rpm.

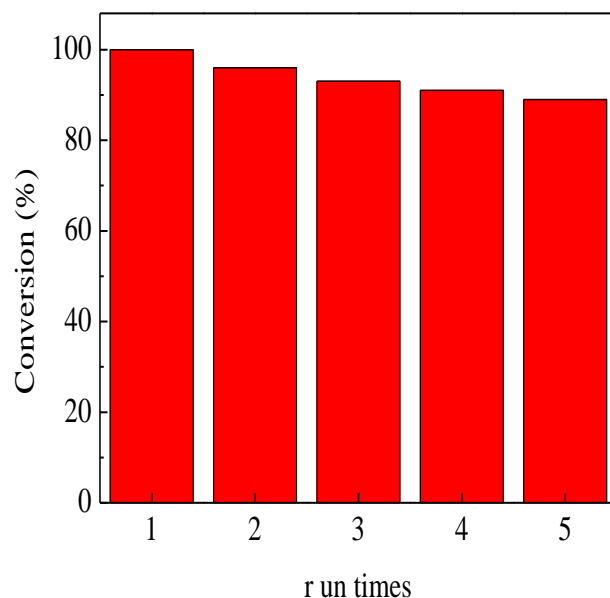


Fig. 8. The conversion of recycled catalyst (Pd-IL/AC-cr)

Reaction conditions: 0.05 g catalyst, 10 mL (8 g/L, 4-CP) + 10 mL (1 mol/L HCOOH + 0.8 mol/L HCOONa), Time = 2 h, Temperature = 306 K, Stirring rate = 600 rpm.

Furthermore, the improved catalytic activity of Pd-IL/AC-cr over Pd-IL/AC-c and Pd/AC is further facilitated by better dispersed Pd⁰ species, which is the result of IL effects and active carbon support. First of all, the Pd-IL/AC-cr had higher Pd⁰ loading over Pdⁿ⁺ species evidenced by XPS as shown in Table 1. This directly increased the amount of active center to carry out the HDC reaction. This probably is associated with the electron-deficient nature of the active Pd sites at the Pd nanoparticles.

Secondly, the stronger metal-AC support interactions are evidenced by the binding energy for Pd⁰ components at 336.2 eV, a value 1.3 eV higher than that associated with bulk Pd as shown in Fig. 2(d). This is consistent with the previous study that Pdⁿ⁺ sites could activate the C-Cl bond via abstraction of nucleophilic chloride anion and Pd⁰ sites adsorb the activated H₂ molecules to form Pd-H bonds, which in turn

1
2
3
4 252 would react with nucleophilic Cl^- . Thus, it completes the dechlorination reaction.
5
6
7 253 Therefore, the increased binding energy not only improves the stability of the
8
9 254 catalytic centers but also increases the catalytic active Pd^0 centers.¹⁵
10

11
12 255 Thirdly, the dispersion is facilitated by the IL and reduced the congregation of Pd
13
14 256 nanoparticles. It is well-known that the Pd 3d electronic level binding energy is
15
16
17 257 dependent on the size of the Pd nanoparticles.²⁷ As the diameter of the Pd
18
19 258 nanoparticles decreases, the binding energy of a given component shifts to higher
20
21
22 259 values. The estimated Pd nanoparticle size is estimated at $\sim 3\text{nm}$. The interaction of
23
24
25 260 the Pd centers with the N atoms of IL would form an IL (mono) layer to partially
26
27 261 protect the Pd^0 against oxidation. Such interaction would further be enhanced through
28
29
30 262 the ionic-polar interaction between the Pd centers and IL. Therefore, such interaction
31
32
33 263 with the IL provides the protection and stabilization of Pd nanoparticles.²⁸
34

35 264

37 265 **4 Conclusions**

38
39
40 266 In summary, the modified and stabilized palladium nanoparticles Pd-IL/AC-cr are
41
42
43 267 prepared successfully through calcination and reduction process on active carbon
44
45
46 268 support by using the ionic liquid 1-Butyl-3-methylimidazolium trifluoroacetate. The
47
48
49 269 IL provides a favorable environment for the formation of metal nanoparticles with a
50
51
52 270 small diameter ($\sim 3\text{nm}$) and even-size distribution under mild reaction conditions. The
53
54
55 271 IL plays an important role in stabilizing, dispersing, as well as maintaining the Pd
56
57
58 272 nanoparticles for the HDC reaction of 4-CP. The reduced Pd-IL/AC-cr catalyst is 5~6
59
60 273 times more effective for HDC reaction than Pd-IL/AC-c and Pd/AC catalysts. This

1
2
3
4 274 excellent catalytic activity could be attributed to well disperse nanoparticles, the
5
6 275 reduced Pd species, and the strong interaction between Pd nanoparticles and IL.
7
8
9 276

11 277 **Acknowledgments**

15 278 The project was supported by the National Science Foundation, China
16
17 279 (21506138, 21375092, 21575097 and 21606199), Science and Technology Plan
18
19 280 Project of TaiZhou. HJ Fan gratefully acknowledges the partial financial support by
20
21 281 the U.S. Department of Energy, National Nuclear Security Administration grant
22
23 282 (DE-NA 0001861 & DE-NA 0002630), and the Welch Foundation Grant (#L0002).
24
25
26
27

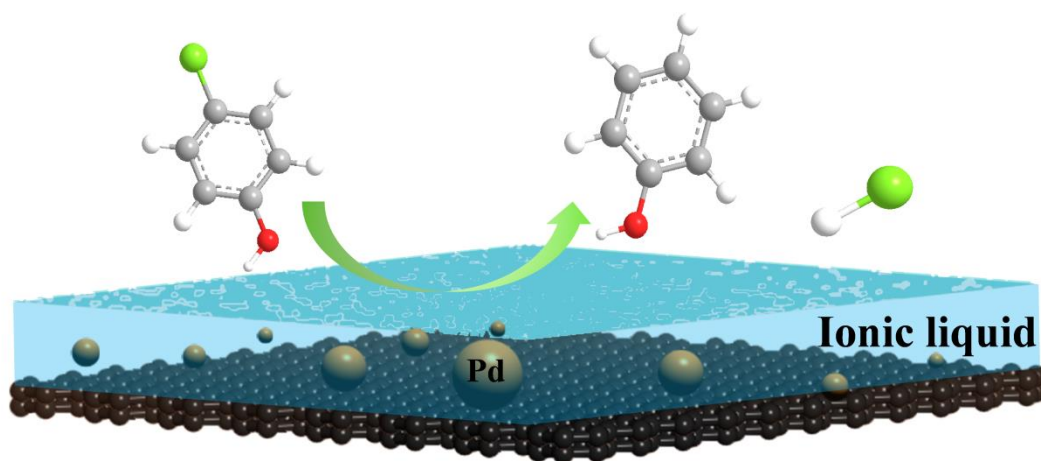
28 283

30 284 **References**

- 32 285 [1] J. Zhao, X. Xu and X. Li, *Catal. Commun.*, 2014, **43**, 102.
33
34 286 [2] Z. Dong, X. Le, C. Dong, W. Zhang, X. Li and J. Ma, *Appl. Catal. B: Environ.*,
35
36 287 2015, **162**: 372.
37
38 288 [3] M. Ming, Y. Ren, M. Hu, Y. Zhang and T. Sun, *Appl. Catal. B: Environ.*, 2017,
39
40 289 **210**, 462.
41
42 290 [4] C. B. Molina, A. H. Pizarro, J. A. Casas and J. J. Rodriguez, *Appl. Catal. B:*
43
44 291 *Environ.*, 2014, 330.
45
46 292 [5] G. Jiang, M. Lan, Z. Zhang, X. Lv, Z. Lou, X. Xu, F. Dong and S. Zhang, *Environ.*
47
48 293 *Sci. Technol.*, 2017, **51**, 7599.
49
50 294 [6] Y. Gao, F. Wang, S. Liao, D. Yu and N. Sun, *Chinese J. Catal.*, 1999, **20**, 236.
51
52 295 [7] Y. Zhang, Y. Shao, H. Chen, H. Wan, Y. Wan and S. Zheng, *Environ. Sci.*, 2012,
53
54
55
56
57
58
59
60

- 1
2
3
4 296 **33**, 88.
5
6
7 297 [8] J. Zhao, W. Bolin and Y. X. Yue, *J. Catal.*, 2018, **365**, 153.
8
9 298 [9] M. Munoz, V. Kolb and A. Lamolda, *Appl. Catal. B. Environ.*, 2017, **218**, 498.
10
11 299 [10] L. M. Gomez-Sainero, X. L. Seoane, J. L. G. Fierro and A. Arcoya, *Catal.*, 2002,
12
13 300 **209**, 279.
14
15
16
17 301 [11] J. Zhao, Y. Yu and X. Xu, *Appl. Catal. B. Environ.*, 2017, **206**, 175.
18
19 302 [12] B. C. Leal, C. S. Consorti, G. Machado and J. Dupont, *Cat. Rev.-Sci. Eng.*, 2015,
20
21 303 **5**, 903.
22
23
24 304 [13] D. Comandella, M. Werheid, F. D. Kopinke and K. Mackenzie, *Chem. Eng. J.*,
25
26 305 2017, **319**, 21.
27
28
29 306 [14] M. Sobota, M. Schmid, M. Happel, M. Amende, F. Maier and H. P. Phys, *Chem.*
30
31 307 *Chem. Phys.*, 2010, **12**, 10610.
32
33
34 308 [15] D. Hulicovajurcakova, A. M. Puziy, O. L. Poddubnaya, F. Suárezgarcía, J. M.
35
36 309 Tascón and G. Q. Lu, *Chem. Soc.*, 2009, **131**, 5026.
37
38
39 310 [16] J. Zhao, Y. Yue, G. Sheng, B. Wang and H. Lai, *Chem. Eng. J.*, 2019, **360**, 38.
40
41
42 311 [17] E. Öchsner, M. J. Schneider, C. Meyer, M. Haumann and P. Wasserscheid, *Appl.*
43
44 312 *Catal. A.*, 2011, **399**, 35.
45
46
47 313 [18] Y. Ding, A. Klyushin, X. Huang, T. Jones, D. Teschner, F. Girgsdies, T. Rodenas,
48
49 314 R. Schlögl and S. Heumann, *Angew. Chem. Int. Ed.*, 2018, **57**, 3514.
50
51
52 315 [19] R. Andreatti, I. D. Somma, R. Marotta,; G. Pinto, A. Pollio and D. Spasiano,
53
54 316 *Water. Res.*, 2011, **45**, 2038.
55
56
57 317 [20] R. Li, J. Zhao, D. Han and X. Li, *Catal. Commun.*, 2017, **97**, 116.
58
59
60

- 1
2
3
4 318 [21] O. M. Ilinitch, F. P. Cuperus, L. V. Nosova and E. N. Gribov, *Catal. Today*, 2000,
5
6 319 **56**, 137.
7
8
9 320 [22] Q. Wang, J. Wang, D. Wang, M. Turhong and M. Zhang, *Chem. Eng. J.*, 2015,
10
11 321 **280**, 158.
12
13
14 322 [23] G. Yuan and M. A. Keane, *Appl. Catal. B: Environ.*, 2004, **52**, 301.
15
16
17 323 [24] J. Wang, H. Liu, X. Gu, H. Wang and D. S. Su, *Chem. Commun.*, 2014, **50**, 9182.
18
19
20 324 [25] B. Xu, L. Yang, F. Zhao and B. Zeng, *Electrochimica Acta.*, 2017, **247**, 657.
21
22 325 [26] C. D. Wanger, W. M. Riggs, L. E. Davis, G. E. Moulder and G. E. Mulenberg,
23
24 326 PerkinElmer Corp.: Waltham, MA., 1979.
25
26
27 327 [27] M. G. Mason, L. J. Gerenser and S. T. Lee, *Phys. Rev. Lett.*, 1977, **39**, 288.
28
29
30 328 [28] H. K. Stassen, R. Ludwig, A. Wulf and J. Dupont, *Chem.*, 2015, **21**, 8324.
31
32 329
33
34
35
36
37
38
39
40
41
42
43
44
45
46
47
48
49
50
51
52
53
54
55
56
57
58
59
60



330